CHEMPHYSCHEM

DOI: 10.1002/cphc.200800034

Infrared Spectroscopy of Dioxouranium(V) Complexes with Solvent Molecules: Effect of Reduction

Gary S. Groenewold,*[a] Michael J. Van Stipdonk,*[b] Wibe A. de Jong,*[c] Jos Oomens,[d] Garold L. Gresham,[a] Michael E. McIlwain,[a] Da Gao,[a] Bertrand Siboulet,[e] Lucas Visscher,[f] Michael Kullman,[b] and Nick Polfer[d]

UO_2^+–solvent complexes having the general formula $[UO_2(ROH)]^+$ (R=H, CH_3, C_2H_5, and n-C_3H_7) are formed using electrospray ionization and stored in a Fourier transform ion cyclotron resonance mass spectrometer, where they are isolated by mass-to-charge ratio, and then photofragmented using a free-electron laser scanning through the 10 μm region of the infrared spectrum. Asymmetric O=U=O stretching frequencies (ν_3) are measured over a very small range [from ~953 cm^{-1} for H_2O to ~944 cm^{-1} for n-propanol (n-PrOH)] for all four complexes, indicating that the nature of the alkyl group does not greatly affect the metal centre. The ν_3 values generally decrease with increasing nucleophilicity of the solvent, except for the methanol (MeOH)-containing complex, which has a measured ν_3 value equal to that of the n-PrOH-containing complex. The ν_3 frequency values for these U(V) complexes are about 20 cm^{-1} lower than those measured for isoelectronic U(VI) ion-pair species containing analogous alkoxides. ν_3 values for the U(V) complexes are comparable to those for the anionic $[UO_2(NO_3)_3]^-$ complex, and 40–70 cm^{-1} lower than previously reported values for ligated uranyl(VI) dication complexes. The lower frequency is attributed to weakening of the O=U=O bonds by repulsion related to reduction of the U metal centre, which increases electron density in the antibonding π orbitals of the uranyl moiety. Computational modelling of the ν_3 frequencies using the B3LYP and PBE functionals is in good agreement with the IRMPD measurements, in that the calculated values fall in a very small range and are within a few cm^{-1} of measurements. The values generated using the LDA functional are slightly higher and substantially overestimate the trends. Subtleties in the trend in ν_3 frequencies for the H_2O–MeOH–EtOH–n-PrOH series are not reproduced by the calculations, specifically for the MeOH complex, which has a lower than expected value.*

1. Introduction

Accurate prediction of structure and reactivity of actinide complexes represents one of the frontiers of theoretical chemistry.[1,2] The advance of computational chemistry in accommodating calculations of f-element complexes and clusters has been remarkable,[3–6] and yet the large numbers of electrons involved, the complexity of the electronic structure, relativistic effects, and the possibility of spin–orbit coupling combine to challenge current computational strategies.[4,5] This challenge takes on added significance because of the need to design and synthesize next-generation complexing agents capable of functioning in advanced separations processes[7–12]—an area in which theoretical chemistry plays an important role.

One of the general objectives is to develop a detailed understanding of what occurs when solvent molecules attach to metal centres, both in terms of binding strength, type of bonding and influence on other ligands. Using a trapped-ion mass spectrometer (TrIMS) is an attractive approach for examining these phenomena, because it enables single species to be studied as solvent molecules are added. For example, we have previously studied how dioxouranium species added water, acetone, nitriles and dioxygen.[13,14] But the limitation of a TrIMS approach is that only mass-to-charge values are measured, and the structure must be inferred from chemical intuition or from theoretical chemistry.

Recently, we have shown that TrIMS can be combined with infrared multiple photon dissociation (IRMPD) spectroscopy to determine the structures of f-element complexes.[15–18] Using this technique, discrete metal–ligand species are formed and isolated in explicitly defined solvation states. These complexes

[a] Dr. G. S. Groenewold, Dr. G. L. Gresham, Dr. M. E. McIlwain, Dr. D. Gao
Chemical Sciences, Idaho National Laboratory
2151 North Blvd., Idaho Falls, ID, 83415-2208 (USA)
Fax: (+1) 208 526 8541
E-mail: gary.groenewold@inl.gov

[b] Prof. M. J. Van Stipdonk, M. Kullman
Department of Chemistry, Wichita State University, Wichita, KS (USA)
Fax: (+1) 316 978 3431
E-mail: mike.vanstipdonk@chemistry.wichita.edu

[c] Dr. W. A. de Jong
Environmental Molecular Sciences Laboratory
Pacific Northwest National Laboratory, Richland, WA (USA)
Fax: (+1) 509 376 0420
E-mail: wibe.dejong@pnl.gov

[d] Dr. J. Oomens, Prof. N. Polfer
FOM Instituut voor Plasmafysica Rijnhuizen, Nieuwegein (The Netherlands)

[e] Dr. B. Siboulet
DEN/DRCP/SCPS, CEA Marcoule, 30207, Bagnols-sur-Cèze Cedex (France)

[f] Prof. L. Visscher
Vrije Universiteit Amsterdam (The Netherlands)

Supporting information for this article is available on the WWW under http://www.chemphyschem.org or from the author.

are irradiated using a high-intensity free-electron laser, which is tuneable through the mid-infrared wavelength range. The complexes absorb tens to >100 photons when the wavelength of the laser is in resonance with a fundamental, and the energy deposited is randomized within the complex by internal vibrational energy redistribution. The energized complexes can then dissociate, most commonly by elimination of a neutral solvent molecule, concurrently producing a fragment ion.[19–28] An IRMPD spectrum is generated by recording photofragment peak intensities as a function of wavelength, and these spectra have been shown to bear close resemblance to direct absorption spectra.[18]

Actinide complexes containing the uranyl molecule $[UO_2]^{2+}$ are nearly ideal systems for IRMPD study because the asymmetric stretch (ν_3) of the linear O=U=O moiety is sensitive to equatorial coordination. Donation of electron density to the uranium metal centre causes repulsion of the axial oxo ligands that is observable as a red shift in the IRMPD spectrum. Promotion of an electron into an excited state also reduces the ν_3 frequency.[2] Our previous studies showed that ν_3 is shifted to lower values by 1) increasing the number of equatorial ligands, or 2) increasing the nucleophilicity of the ligands.[15,17] The frequency values for solvent-ligated $[UO_2]^{2+}$ and $[UO_2(anion)]^+$ complexes approached those measured in solution,[29,30] but were in general slightly higher. This difference was interpreted in terms of additional solution-phase interactions that were not occurring in the gas phase, that is, additional equatorially-bound ligands[31,32] or interaction of acids with the axial oxo ligands.[33] The experimental values for the uranyl complexes were also compared with those generated using density functional theory (DFT) methods.[34–36] In general, the computational accuracy was very good, within a few, or at most 20 cm^{-1} of the measurements.[15,17,18]

The influence of electron-donating neutrals and anions on the uranyl ν_3 frequency motivated interest in the effect of formal reduction of the uranium atom. Addition of an electron represents the ultimate in contribution of electron density to the metal centre. Complexes containing $[UO_2]^+$, a U(V) species which is formally $5f^1$, have been difficult to study because of their tendency to undergo disproportionation and oxidation in solution.[37] Mizuoka and Ikeda showed that reduction significantly reduces uranyl stretching frequencies.[38,39] Even earlier, Jones and Penneman measured the ν_3 value for $[NpO_2]^{2+}$ in a non-complexing perchlorate solution.[30] This $5f^1$ species was probably a penta-aquo complex, and it produced a ν_3 value of 969 cm^{-1}, which is slightly higher than the value for the $5f^0$ value of 965 cm^{-1} measured for penta-aquo $[UO_2]^{2+}$. Matrix isolation spectroscopy (MIS) has also been used effectively to study $[UO_2]^+$. MIS avoids problems with disproportionation and reduces the complexity of solvent interactions, because frequencies are measured in frozen noble gases. A peak at 892.3 cm^{-1} measured using MIS was assigned to the ν_3 stretch of the $[(UO_2^+)(O_2^-)]$ ion pair,[40] and further MIS studies produced $[UO_2]^+$ ν_3 values that were clearly altered by the solid noble gas environment.[41] The ν_3 frequency of $[UO_2(Ne)_6]^+$ was measured at 980.1 cm^{-1}, and pentavalent complexes with Ar, Kr and Xe were recorded at 952.3, 940.6, and 929.0 cm^{-1}, respectively, indicating that the noble gases were forming coordination complexes with $[UO_2]^+$.[42] These measurements provided an excellent opportunity for rigorous comparisons with the results of theoretical calculations; for example, work by Majumdar indicated that for $[U(V)O_2]^+$, results using the hybrid B3LYP functional produced the most accurate frequencies, although alternative methods could also be used effectively.[43]

Recently, we discovered that solvent complexes of the reduced uranyl molecule $[UO_2]^+$ can readily be formed by increasing the harshness of the electrospray ionization used to transit uranyl complexes from solution into the gas phase of a trapped ion mass spectrometer. The presence of U(V) complexes was indicated by formation of ions having *m/z* values corresponding to the general formula $[UO_2(solvent)]^+$, which contrasted with *m/z* values for $[UO_2(solvent)_n]^{2+}$ and $[UO_2(anion)]^+$ species [both U(VI)],[15,17] and strongly indicating the presence of the V state. This conclusion was bolstered by very different dioxygen reactivities of the $[UO_2(solvent)_n]^+$ complexes, which were distinct from that of isoelectronic U(VI) species.[44] The formation of the $[UO_2(solvent)]^+$ complexes offered the possibility of acquiring IRMPD spectra for these U(V) species. The spectra enabled comparisons with an initial set of frequency calculations that were performed using functional–basis set combinations that had previously been shown to be effective for heavy element coordination complexes. Herein we report measured and calculated frequencies for $[UO_2]^+$ ligated with a single solvent molecule, either H_2O, MeOH, EtOH or *n*-PrOH.

2. Results and Discussion

2.1. IRMPD Measurements

Electrospray ionization of solutions of uranyl nitrate containing various solvent molecules produce a variety of complexes depending on the conditions of the ESI source. When the desolvation gas temperatures are kept low, the abundant ions in the ESI spectrum are uranyl complexes that are extensively solvated with either acetone and or acetonitrile, and have general compositions that correspond to $[UO_2(neutral)_n]^{2+}$ where $n=4$ or 5.[13,15] When the desolvation gas temperature of the ESI source is raised slightly above ambient, the dominant species in the positive ion mass spectrum are $[UO_2(anion)(neutral)_n]^+$, where $n=1$–2.[17] Raising the desolvation temperature to about 50 °C results in observation of mainly $[UO_2(solvent)]^+$ species, in which the metal atom is in the V oxidation state.[44] The observation of the $[UO_2(solvent)]^+$ complexes is key to this IRMPD study, because while unligated $[UO_2]^+$ is formed, the oxygen ligands are very tightly bound, making it impossible to photodissociate the bare $[UO_2]^+$ under the irradiation conditions employed here. For a tightly bound molecule like $[UO_2]^+$, employing a tagging strategy that utilizes a weakly bound neutral is effective for measuring the vibrational frequencies.[19,45,46] Infrared absorption leads to the detachment of the weakly bound neutral by photofragmentation (Scheme 1).

In the case of the *n*-propanol complexes, a competing photofragmentation is observed in which the alcohol undergoes

Scheme 1. IRMPD elimination of ROH from $[UO_2(ROH)]^+$ complexes.

rearrangement followed by loss of propene (Scheme 2). The formation of $[UO_2(H_2O)]^+$ by this elimination reaction provides the opportunity to examine the IRMPD spectrum of the mono-

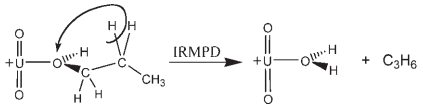

Scheme 2. IRMPD elimination of propene from $[UO_2(n\text{-}C_3H_7OH)]^+$ complexes.

aquo complex. In these experiments, the elimination of propene is accomplished by collision-induced dissociation of the propanol complex, followed by isolation of $[UO_2(H_2O)]^+$ for subsequent IRMPD.

The salient feature is the asymmetric O=U=O stretching frequency ν_3, which appears in the IRMPD spectra of all four complexes (Table 1, Figure 1). The frequency maxima values for all four complexes are generated by fitting a Gaussian curve through the data. The ν_3 values for the four complexes fall over a very small frequency range of only 8 cm^{-1}; the peak for the H_2O complex is distinctively higher compared to those for the three alcohol complexes, which are within 4 cm^{-1} of each other. We believe that these small frequency differences are near, or at the limit, of what can be distinguished using FELIX, although the precision of the ν_3 measurements is not rigorously established, because beam time is scarce and spectral acquisition requires two to four hours. Together, these factors militate against collecting another set of acquisitions. However the ordering of ν_3 values for these four complexes is likely correct. This conclusion is inferred from prior measurements of ν_3 values for $[UO_2(acetone)_n(acetonitrile)_m]^{2+}$ complexes.[15] In two sets of complexes ($n+m=3$, 4) substitution of the more nucleophilic acetone for the less nucleophilic acetonitrile always result in a red shift, the smallest of which is 3 cm^{-1}. This is exactly what should occur, and indicates that differences of only a few cm^{-1} can accurately be distinguished. This suggests that in the present case, the relative order of the ν_3 values for the complexes follows the order *n*-PrOH < MeOH < EtOH < H_2O (as shown in Figure 1). The signal-to-noise ratio for the *n*-PrOH and EtOH complexes is excellent, lending a high level of confidence to these measurements. The peak for the MeOH complex is a bit noisier, but nevertheless the sides of the peak and its centroid are slightly lower than those of the EtOH complex, and are nearly as low as the *n*-PrOH complex.

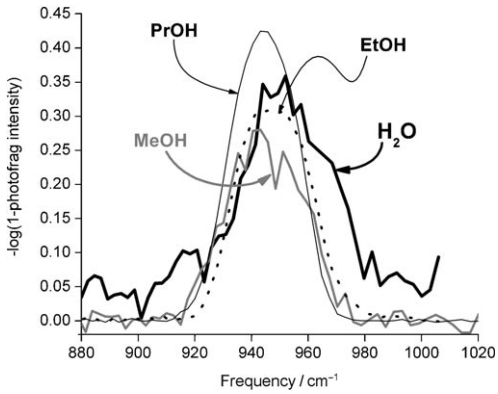

Figure 1. IRMPD spectra of the asymmetric O=U=O stretch for isolated $[UO_2(ROH)]^+$ complexes.

The order of the ν_3 values for the complexes is surprising, because uranyl frequencies are generally shifted to lower values as donation of electron density from the ligands increases.[15–18] A priori, we expect that stronger nucleophilic ligands would progressively shift to lower uranyl ν_3 frequencies, following the general order $[UO_2(PrOH)]^+ < [UO_2(EtOH)]^+ < [UO_2(MeOH)]^+ < [UO_2(H_2O)]^+$, which is the inverse of the order of their proton affinities (PA).[47] We compare the red shifts caused by the solvents with PA values because experimental binding energy data for the UO_2^+–solvent species are not available, and PAs have been shown to follow the same trend as alkali cation nucleophilicities.[48] The inverse correlation between ligand PAs and uranyl ν_3 values is seen in the prior IRMPD measurements of the uranyl dication ligated with acetonitrile and acetone—the latter has a PA that is 7.8 kcal mol^{-1} higher,[47] and substitution of acetone for acetonitrile results in a red shift of the ν_3 frequency by ~3–7 cm^{-1}.[15] A similar correlation is partially observed for the $[UO_2(ROH)]^+$ complexes (Figure 2). Compared to H_2O, EtOH has a PA that is 20.6 kcal mol^{-1} higher, and a ν_3 red shifted by 4 cm^{-1}. Similarly, *n*-PrOH has a PA that is 2.4 kcal mol^{-1} higher than that of EtOH, and a ν_3 red shifted by another 4 cm^{-1}. The exception to the trend is MeOH, which has a PA that is 7.7 kcal mol^{-1} less than that of *n*-PrOH, but a ν_3 frequency that is about the same. We believe that this inconsistency is reconciled by overlapping vibrational modes, as suggested by DFT calculations described herein.

The $[UO_2(ROH)]^+$ complexes are close U(V) analogues to corresponding U(VI) complexes $[UO_2(RO)]^+$, where the anion RO^- is the deprotonated form of the

Table 1. O=U=O asymmetric stretching frequencies for U(V) species $[UO_2(ROH)]^+$, compared with values for analogous U(VI) ion pair species having formulae $[UO_2(RO)]^+$ and $[UO_2(RO)(H_2O)]^+$. The U(VI) values have been reported in a prior publication.[17]

U(V) Species	UO_2 asym freq [cm^{-1}]	U(VI) alkoxide species	UO_2 asym freq. [cm^{-1}]	Hydrated U(VI) oxide species	UO_2 asym. freq. [cm^{-1}]
$[UO_2(H_2O)]^+$	952	$[UO_2(OH)]^+$	971	$[UO_2(OMe)(H_2O)]^+$	970
$[UO_2(MeOH)]^+$	945	$[UO_2(OMe)]^+$	966	$[UO_2(OH)(H_2O)]^+$	983
$[UO_2(EtOH)]^+$	948	$[UO_2(OEt)]^+$	–	$[UO_2(OAc)(H_2O)]^+$	993
$[UO_2(PrOH)]^+$	944	$[UO_2(OPr)]^+$	964		

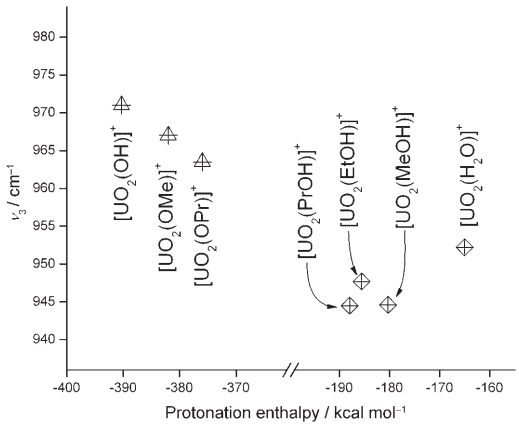

Figure 2. Comparison of ν_3 frequencies measured for $[U(V)O_2(ROH)]^+$ complexes (◇) compared with analogous $[U(VI)O_2(RO)]^+$ complexes (△). Values are plotted versus proton affinities for the neutral alcohols and the analogous alkoxides.[47]

ROH solvent ligands. Values for $[UO_2OMe]^+$ and $[UO_2OH]^+$ have been measured in a previous study,[17] and we are able to measure the IRMPD of $[UO_2(n\text{-PrO})]^+$ via its photoelimination of C_3H_6, which peaks at 963.5 cm^{-1}. In general, moving from the uranyl alkoxide cations to the analogous $[U(V)O_2(ROH)]^+$ species results in red shifts on the order of 18 to 21 cm^{-1}, which arise from a combination of the opposing effects of replacing the alkoxide with the alcohol (shifting ν_3 to the blue) and the formal reduction of the U centre (shifting ν_3 even further to the red). Interestingly, the trend for the anion complexes is opposite to that of the neutrals, in that the weakest conjugate base,[47] $n\text{-PrO}^-$, produces the largest ν_3 red shift, while conversely the strongest nucleophile, OH^-, produces the smallest shift (Figure 2).

Prior measurements of the ν_3 values for hydrated complexes of U(VI) species having the general composition $[UO_2(\text{anion})(H_2O)]^+$ enable comparisons of different anions[17] versus the electron present at the U centre in the $[UO_2(H_2O)]^+$ complex. This shows that compared to $[UO_2(\text{anion})(H_2O)]^+$ complexes with either OAc^-, OH^-, or MeO^- anions, the ν_3 value for the $[UO_2(H_2O)]^+$ complex is shifted to a significantly lower frequency and that the magnitude of the red shift follows the order $OAc^- < OH^- < OMe^- < e^-$.

2.2. DFT Calculations

Initial density functional theory calculations are conducted using LDA/DSPP/DNP, which in past studies of $U(VI)O_2^{2+}$ complexes (f^0 systems) with varying anionic ligands have produced good agreement with ν_3 trends.[17,18] Herein, the LDA-calculated ν_3 value for the $[UO_2(PrOH)]^+$ complex agrees with IRMPD (Table 2); however, values calculated for the other three complexes are higher than the measurements, by as much as 18 cm^{-1} in the case of the H_2O complex. Furthermore, LDA dramatically over-predicts the shift ($\Delta\nu_3$) upon substitution of ligands having differing nucleophilicities. The LDA calculations predict that the uranyl ν_3 frequencies should be red shifted and that the magnitude of the shifts should increase following the order $[UO_2(PrOH)]^+ > [UO_2(EtOH)]^+ > [UO_2(MeOH)]^+ > [UO_2(H_2O)]^+$, which is in line with expectations.

Better agreement is achieved performing calculations using the hybrid B3LYP functional, particularly using the LANL2dz ECP and aug-cc-pVDZ basis set (Table 2). The calculated ν_3 values are all within 4 cm^{-1} of the IRMPD measurements, with $\Delta\nu_3$ being 5 cm^{-1} upon going from H_2O to MeOH, and MeOH to EtOH. Surprisingly, the calculated ν_3 value of the *n*-PrOH complex is slightly higher than that of EtOH, even though propanol is expected (and calculated) to bind more strongly (Table 3, and crossed data points in Figure 3).

The B3LYP calculations are checked against values generated using the PBE functional, employing two different approaches with respect to the basis set and the treatment of the core electrons. Employing the SDD/TZVP basis set, ν_3 values are within 9 cm^{-1} of the IRMPD measurements, and has $\Delta\nu_3$ values that are 9 and 4 cm^{-1} on going from H_2O to MeOH and MeOH to EtOH, respectively. The PBE/SDD/TZVP ν_3 values follow the same trend, including a value for the *n*-PrOH complex that is slightly higher than that of the EtOH complex. Comparison of the PBE/SDD/TZVP calculations for the $[UO_2(ROH)]^+$ complexes with the analogous isoelectronic U(VI) alkoxide species $[UO_2(OR)]^+$ shows a red shift upon reduction of the uranium metal centre that is in the order of 20 cm^{-1}, in good agreement with the IRMPD data (see Table S1 of the Supporting Information).

Table 2. O=U=O asymmetric stretching frequencies (ν_3, cm^{-1}) measured for [U(V)] species $[UO_2(ROH)]^+$ using IRMPD, compared with calculated frequencies.

Complex	Experimental ν_3 IRMPD	Theoretical ν_3 LDA/DSPP/DNP	B3LYP/LANL2dz/ aug-cc-pVDZ	PBE/ZORA/TZ2P	PBE/SDD/TZVP
$[UO_2(H_2O)]^+$	952	970	954	960	961
$[UO_2(MeOH)]^+$	945	963	949	947	952
$[UO_2(EtOH)]^+$	948	957	944	–	948
$[UO_2(PrOH)]^+$	945	944	945	–	949

Table 3. O=U=O asymmetric stretching frequencies (ν_3, cm^{-1}) measured for [U(V)] species $[UO_2(ROH)]^+$ using IRMPD, compared with calculated binding energies (kcal mol^{-1}).

Complex	Experimental ν_3 IRMPD	Calculated Binding Energy [kcal mol^{-1}] B3LYP/LANL2dz/aug-cc-pVDZ	PBE/ZORA/TZ2P	PBE/SDD/TZVP
$[UO_2(H_2O)]^+$	952	33.4	41.3	36.6
$[UO_2(MeOH)]^+$	945	41.1	42.9	40.7
$[UO_2(EtOH)]^+$	948	42.7	–	43.3
$[UO_2(PrOH)]^+$	945	44.0	–	44.1

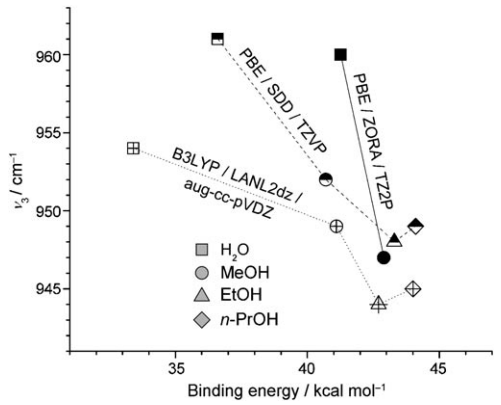

Figure 3. DFT-calculated uranyl ν_3 values versus calculated binding energies.

Calculations using PBE/ZORA/TZ2P employ a different approach for handling the core electrons, and produce similar values for the H_2O and MeOH complexes to those generated using PBE/SDD/TZVP. The $\Delta\nu_3$ on substituting MeOH for H_2O is 13 cm^{-1}—thus greater than that calculated using the other methods. We were unsuccessful in finding the minimum energy structures for the EtOH and *n*-PrOH complexes using the ZORA/TZ2P basis

In all calculations scalar relativity is accounted for and effects due to spin–orbit coupling are ignored. Inclusion of spin–orbit operators for $[UO_2H_2O]^+$ increases the ν_3 by 5-8 cm^{-1}, depending on the operator used (Supporting Information, Table S2). While spin–orbit effects may lead to a small shift in the vibrational frequencies, differential effects among the studied species are anticipated to be much smaller due to the compact nature of the uranium 5f^1 orbital and its limited contribution to ligand bonding.

As in the case of the IRMPD data, the ν_3 values calculated using both B3LYP/LANL2dz/aug-cc-pVDZ and PBE/SDD/TZVP are within a few cm^{-1} of one another for the three alcohol complexes. This suggests that alterations to the hydrocarbon chain are not significantly affecting the interaction of the hydroxy functional group with the $[UO_2]^+$ centre, a conclusion that is consistent with the relative binding energies calculated for the complexes. The calculated binding energies become stronger following the expected order $H_2O < MeOH < EtOH < n$-PrOH (Table 3). These values and their order are very similar to those measured for Li^+,[48] indicating that like Li^+, $[UO_2]^+$ behaves as a hard cation, functioning as an aggressive Lewis acid. The largest increase in binding energies occurs upon going from H_2O to MeOH, with smaller changes upon going to EtOH and *n*-PrOH, which is consistent with the general pattern of the ν_3 measurements.

The fact that the DFT functionals predict a trend of decreasing uranyl ν_3 frequency with increasing binding energy and/or PA focuses our attention on why MeOH behaves anomalously in the IRMPD measurements. The ν_3 value for $[UO_2(MeOH)]^+$ should be greater than that of the EtOH complex, but less than that of the H_2O complex. One explanation is that for both the EtOH and MeOH complexes, lower intensity vibrational modes of the ligands overlap with the uranyl ν_3, altering its apparent peak position in the IRMPD measurement. The PBE/SDD/TZVP calculations reveal a C–O stretch at 924 cm^{-1} for the MeOH complex, and overlapped C–C and C–O stretches with a C–H wag centred at 968 cm^{-1} for the EtOH complex. These peaks, which would not be expected to be resolved from the asymmetric uranyl fundamental, might shift the apparent uranyl ν_3 for $[UO_2(MeOH)]^+$ (expected at 952 cm^{-1}) to a lower value, and the ν_3 for $[UO_2(EtOH)]^+$ to a higher value. Vibrational modes calculated for the *n*-PrOH complex are similar to those of the EtOH complex, but the predicted values are well to the red of the ν_3 frequency. As the H_2O complex does not have these vibrations, neither the *n*-PrOH nor the H_2O complexes should be affected. Similar trends are found for the B3LYP/LANL2dz/aug-cc-pVDZ calculations. When we convoluted the predicted ligand vibrational frequencies with the uranyl ν_3, the peak position for the MeOH complex is unchanged at 952 cm^{-1}, while that of the EtOH complex is slightly shifted to the blue (coincidently also to 952 cm^{-1}, Supporting Information, Figure S1). Therefore the peak position of the MeOH complex is not likely to be influenced by ligand vibrational modes, and the experimental trend in ν_3 values is not yet accounted for by our modelling.

The structures generated by the DFT calculations for the $[UO_2(ROH)]^+$ complexes display substantial similarity, as indicated in Figure 4, and Table S3 in the Supporting Information.

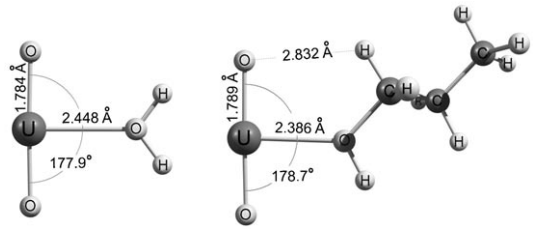

Figure 4. Structures calculated for $[UO_2(H_2O)]^+$ (left) and $[UO_2(n\text{-PrOH})]^+$ (right), using PBE/SDD/TZVP.

All calculations indicate a nearly linear O=U=O moiety, contrasting with the $[U(VI)O_2(anion)]^+$ complexes in which attachment of an anion to the uranyl metal centre causes perturbation of the linear O–U–O angle (to ~170°).[17] The comparison suggested that the perturbation seen in the $[U(VI)O_2(anion)]^+$ complexes is largely counteracted by the non-bonding electron at the uranium metal centre in the $[U(V)O_2(solvent)]^+$ complexes.

The calculations show that the $r_{O=U}$ distances lengthen, and that the r_{U-OHR} shorten as the ligand changes from H_2O to MeOH to EtOH to *n*-PrOH (Table S2). This is consistent with the trends calculated for the uranyl ν_3 frequencies and binding energies.

Structures generated using the PBE/SDD/TZVP approach indicate that the ROH ligands align parallel to the O=U=O moiety, as shown in Figure 4 for the H_2O and *n*-PrOH complexes. The O–U–O–C dihedral angles in the alcohol complexes are $\leq 4°$ in most calculations. Generally, the H atom attached to the α-carbon adopts a position proximate to the

uranyl oxygen (~2.8 A), suggesting that a weak interaction may be in part responsible for this conformation. For the B3LYP and LDA calculations, the orientation of the carbon atoms in the larger alcohols is closer to the equatorial plane.

3. Conclusions

Recent spectroscopic investigations of discrete uranyl coordination complexes isolated in the vacuum environment of a trapped ion mass spectrometer have resulted in IR spectra that are highly diagnostic for complex structures, and enable direct comparisons with computational results without having to account for solvent influence. However, the frontier lies in investigations of actinide complexes containing multiple non-bonding f electrons in the valence shell. These complexes promise to display a more diverse array of chemistry, and thus provide a challenge for computational methods. Therefore, spectroscopic measurements on discrete complexes containing non-bonding f electrons are needed in order to facilitate improved understanding of bonding and to assist in benchmarking calculations. Herein, we reported IR frequencies of the asymmetric UO_2 stretch (ν_3), of discrete $[U(V)O_2]^+$ solvent complexes involving H_2O, MeOH, EtOH and *n*-PrOH. The ν_3 values show red shifting of about 20 cm^{-1} compared to ν_3 values of analogous isoelectronic $[UO_2]^{2+}$ complexes [U(VI) species that contain no non-bonding f electrons]. The ν_3 values for the U^V species are comparable to those recently reported for uranyl [U(VI)] ligated to three anions.[18]

Differences in the ν_3 values of the four complexes are small, indicating that altering the alkyl group does not significantly affect the metal centre. In comparing the four different complexes, a subtle trend observed in comparing the ν_3 frequencies is one of decreasing values with increasing ligand nucleophilicities. However, the value for the MeOH-containing complex is as low as that of *n*-PrOH. Frequencies calculated using different DFT methods are in good general agreement with IRMPD, and each computational approach predicts a decreasing uranyl ν_3 frequency with increasing ligand PA. The best agreement was achieved using B3LYP/LANL2dz/aug-cc-pVDZ, a conclusion similar to that reported by Majumdar.[43] However none of the approaches reproduced the subtleties of the experimental (IRMPD) trend of uranyl ν_3 frequencies related to the relative position of the MeOH and EtOH complexes. It may be that studies of f^1 complexes containing a ligand series with a more pronounced range of nucleophilicities would provide a better platform against which DFT approaches can be evaluated, and these will be emphasized in future work.

Experimental Section

IRMPD spectra were collected at the Free Electron Laser for Infrared eXperiments (FELIX) facility, located at the FOM Instituut voor Plasmafysica "Rijnhuizen" (Nieuwegein, The Netherlands).[24] The free electron laser is interfaced to a Fourier transform ion cyclotron resonance (FT–ICR) mass spectrometer.[23]

Generation of Uranyl Complexes by Electrospray Ionization Fourier Transform Ion Cyclotron Resonance Mass Spectrometry (ESI–FT–ICR–MS):[22,23,27] An ESI source (Z-spray, Micromass, Manchester, U.K.) operated at ~3 kV was used to generate singly-charged complexes of $[UO_2]^+$ that contained one solvent molecule.[13,49] A 1 mM solution of uranyl nitrate (Fluka/Sigma–Aldrich, St. Louis, MO, USA) in water was used to produce the uranyl complexes that were accumulated for between 500 and 1000 ms in a hexapole ion trap, prior to being gated into the FT–ICR–MS. The mass spectra were sensitive to the temperature of the N_2 desolvation gas used in the ESI source.[13] The desolvation temperature was controlled by a heater and thermocouple at 52 °C; note that when lower temperatures were used, U(VI) complexes were formed.[15,17] The oxidation state was also sensitive to the extraction voltage applied to the sampling cone, and this was tuned to maximize formation of the U^V species on an as-needed basis. The flow rates of the spray solution and the desolvation gas were maintained at 25 μL min^{-1} and 30 L min^{-1}, respectively. Complexes selected for IRMPD interrogation were isolated using a stored waveform inverse Fourier transform (SWIFT) pulse,[50] which ejected all species except those having the desired mass.

Infrared Multiphoton Dissociation (IRMPD): Isolated ionic complexes were irradiated using two FELIX macropulses, which induced elimination of a solvent molecule from the complex when the incident wavelength matched an absorption band. The IRMPD mechanism has been described in detail elsewhere.[51] Briefly, it involves sequential, non-coherent absorption of many (tens to hundreds) infrared photons, with each photon being relaxed by intramolecular vibrational redistribution before the next one is absorbed. In this way, the internal vibrational energy of the molecule can resonantly be increased above the dissociation threshold, resulting in fragmentation. It has been shown that the infrared spectra obtained are comparable to those obtained using linear absorption techniques.[27,28] FELIX was scanned between ~9.8–11.2 μm in increments $\leq$0.04 μm, after which IRMPD product ions and undissociated precursor ions were measured using the excite/detect sequence of the FT–ICR–MS.[52,53] The IRMPD efficiency was then expressed as -log[1-(summed fragment ion yield)], corrected for the width of the acquisition channels and linearly normalized to correct for variations in FELIX power over the spectral range. The spectra of all four complexes were acquired in a single shift, to maintain calibration consistency.

DFT Structure and Frequency Calculations: DFT calculations of structures and harmonic frequencies were performed with the DMol^3,[54,55] NWChem,[56,57] and ADF2006.01[58] suites of programs. Different combinations of functionals, basis sets, and relativistic treatments were employed in efforts to derive a consistent view of the IRMPD phenomena measured in the context of complex structure and dissociation behaviour: 1) In DMol^3 the local density approximation (LDA) with the Vosko, Wilk and Nusair (VWN) parameterization[59,60] was employed using the density functional semicore pseudopotential (DSPP).[61] This accounts for scalar relativistic effects and includes 60 electrons in the uranium core (comparable to Stuttgart/Dresden small core ECPs). The pseudopotentials employed in the DMol^3 calculations include spin orbit considerations. Polarized numerical basis sets (DNP) were used for the active electrons. 2) In NWChem the hybrid B3LYP functional[62,63] was used, with uranium described using the LANL2dz ECP and orbital basis set.[64] Other atoms in the complexes (O, C, and H) were described using the aug-cc-pVDZ orbital basis sets.[65] Calculations were also performed using the PBE functional[66,67] (a generalized gradient approximation). In these calculations, the MWB60 ECP and basis set (SDD/TZVP)[68–71] was used, which features Stuttgart/Dresden effective core potentials. For the spin–orbit calculations, the oxygen

basis was replaced by the CRENBL ECP and associated basis set.[72] A very fine grid and very tight convergence criteria for both energy and geometry optimization were used throughout the calculations with NWChem. For DFT energies, convergence was set to $1.0d^{-8}$, and an xfine grid was used. 3) In ADF2006.01 the scalar relativistic ZORA[73] Hamiltonian combined with the TZ2P type basis set was applied within the framework of unrestricted DFT, the PBE functional and a frozen core including the 5d electrons. This adds up to 78 electrons. Vibrational frequencies were calculated analytically.

Acknowledgements

Work by G. S. Groenewold, G. L. Gresham, Da Gao and M. E. McIlwain was supported by the U.S. Department of Energy, INL Laboratory Directed Research & Development Program under DOE Idaho Operations Office Contract DE-AC07-05ID14517. M. J. Van Stipdonk was supported through a grant from the U. S. National Science Foundation (NSF grant CAREER-0239800). The FOM authors were supported by the Nederlandse Organisatie voor Wetenschappelijk Onderzoek. The skillful assistance by the FELIX staff, in particular Dr. B. Redlich, is gratefully acknowledged. Construction and shipping of the FT–ICR–MS instrument was made possible through funding from the National High Field FT–ICR Facility (grant CHE-9909502) at the National High Magnetic Field Laboratory, Tallahassee, FL. W. A. de Jong's research was supported by the BES Heavy Element Chemistry program of the U.S. Department of Energy, Office of Science, and was performed in part using the Molecular Science Computing Facility in the William R. Wiley Environmental Molecular Sciences Laboratory, a national scientific user facility sponsored by the U.S. Department of Energy's Office of Biological and Environmental Research located at the Pacific Northwest National Laboratory, which is operated for the Department of Energy by Battelle. L. Visscher thanks the Netherlands Organization for Scientific Research (NWO) for financial support through the VICI program. B. Siboulet was supported by the Commissariat à l'Energie Atomique DSOE/RB program.

Keywords: density functional calculations · infrared multiple photon dissociation spectroscopy · mass spectroscopy · uranium · uranyl coordination complex

[1] M. Pepper, B. E. Bursten, *Chem. Rev.* **1991**, *91*, 719–741.
[2] R. G. Denning, *Struct. Bond.* **1992**, *79*, 215–276.
[3] N. Kaltsoyannis, *Chem. Soc. Rev.* **2003**, *32*, 9–16.
[4] G. Schreckenbach, P. J. Hay, R. L. Martin, *J. Comput. Chem.* **1999**, *20*, 70–90.
[5] C. Van Wüllen, *J. Comput. Chem.* **1999**, *20*, 51–52.
[6] V. Vetere, P. Maldivi, C. Adamo, *J. Comput. Chem.* **2003**, *24*, 850–858.
[7] G. Choppin, *Radiochim. Acta* **2004**, *92*, 519–523.
[8] H. Eccles, *Solv. Extr. Ion Exch.* **2000**, *18*, 633–654.
[9] J. N. Mathur, M. S. Murali, K. L. Nash, *Solv. Extr. Ion Exch.* **2001**, *19*, 357–390.
[10] K. L. Nash, *Solv. Extr. Ion Exch.* **1993**, *11*, 729–768.
[11] K. L. Nash, R. E. Barrans, R. Chiarizia, M. L. Dietz, M. P. Jensen, P. G. Rickert, *Solv. Extr. Ion Exch.* **2000**, *18*, 605–631.
[12] A. P. Paiva, P. Malik, *J. Radioanal. Nucl. Chem.* **2004**, *261*, 485–496.
[13] M. J. Van Stipdonk, W. Chien, V. Angalaban, K. Bulleigh, D. Hanna, G. S. Groenewold, *J. Phys. Chem. A* **2004**, *108*, 10448–10457.
[14] M. J. Van Stipdonk, W. Chien, K. Bulleigh, Q. Wu and G. S. Groenewold, *J. Phys. Chem. A* **2006**, *110*, 959–970.
[15] G. S. Groenewold, A. K. Gianotto, K. C. Cossel, M. J. Van Stipdonk, D. T. Moore, N. Polfer, J. Oomens, W. A. de Jong, L. Visscher, *J. Am. Chem. Soc.* **2006**, *128*, 4802–4813.
[16] G. S. Groenewold, A. K. Gianotto, K. C. Cossel, M. J. Van Stipdonk, J. Oomens, N. Polfer, D. T. Moore, W. A. de Jong, M. E. McIlwain, *Phys. Chem. Chem. Phys.* **2007**, *9*, 596–606.
[17] G. S. Groenewold, A. K. Gianotto, M. E. McIlwain, M. J. Van Stipdonk, M. Kullman, D. T. Moore, N. Polfer, J. Oomens, I. Infante, L. Visscher, B. Siboulet, W. A. de Jong, *J. Phys. Chem. A* **2008**, *112*, 508–521.
[18] G. S. Groenewold, J. Oomens, W. A. de Jong, G. L. Gresham, M. E. McIlwain, M. J. Van Stipdonk, *Phys. Chem. Chem. Phys.* **2008**, *10*, 1192–1202.
[19] M. A. Duncan, *Int. Rev. Phys. Chem.* **2003**, *22*, 407–435.
[20] I. Farkas, I. Banyai, Z. Szabo, U. Wahlgren, I. Grenthe, *Inorg. Chem.* **2000**, *39*, 799–805.
[21] J. Lemaire, P. Boissel, M. Heninger, G. Mauclaire, G. Bellec, H. Mestdagh, A. Simon, S. Le Caer, J. M. Ortega, F. Glotin, P. Maitre, *Phys. Rev. Lett.* **2002**, *89*, 273002.
[22] D. T. Moore, J. Oomens, J. R. Eyler, G. Meijer, G. von Helden, D. P. Ridge, *J. Am. Chem. Soc.* **2004**, *126*, 14726–14727.
[23] D. T. Moore, J. Oomens, L. van der Meer, G. von Helden, G. Meijer, J. Valle, A. G. Marshall, J. R. Eyler, *ChemPhysChem* **2004**, *5*, 740–743.
[24] D. Oepts, A. F. G. van der Meer, P. W. van Amersfoort, *Infrared Phys. Technol.* **1995**, *36*, 297–308.
[25] J. Oomens, D. T. Moore, G. Meijer, G. von Helden, *Phys. Chem. Chem. Phys.* **2004**, *6*, 710–718.
[26] J. Oomens, D. T. Moore, G. von Helden, G. Meijer, R. C. Dunbar, *J. Am. Chem. Soc.* **2004**, *126*, 724–725.
[27] J. Oomens, B. G. Sartakov, G. Meijer, G. von Helden, *Int. J. Mass Spectrom.* **2006**, *254*, 1–19.
[28] J. Oomens, A. G. G. M. Tielens, B. G. Sartakov, G. Von Helden, G. Meijer, *Astrophys. J.* **2003**, *591*, 968–985.
[29] L. H. Jones, *Spectrochim. Acta* **1958**, *10*, 395–403.
[30] L. H. Jones, R. A. Penneman, *J. Chem. Phys.* **1953**, *21*, 542–544.
[31] K. E. Gutowski, D. A. Dixon, *J. Phys. Chem. A* **2006**, *110*, 8840–8856.
[32] G. A. Shamov, G. Schreckenbach, *J. Phys. Chem. A* **2005**, *109*, 10961–10974.
[33] B. Siboulet, C. J. Marsden, P. Vitorge, *Chem. Phys.* **2006**, *326*, 289–296.
[34] Z. Cao, K. Balasubramanian, *J. Chem. Phys.* **2005**, *123*, 114309.
[35] C. Clavaguera-Sarrio, S. Hoyau, N. Ismail, C. J. Marsden, *J. Phys. Chem. A* **2003**, *107*, 4515–4525.
[36] C. Clavaguéra-Sarrio, N. Ismail, C. J. Marsden, D. Begue, C. Pouchan, *Chem. Phys.* **2004**, *302*, 1–11.
[37] J. Selbin, J. D. Ortego, *Chem. Rev.* **1969**, *69*, 657–671.
[38] K. Mizuoka, Y. Ikeda, *Inorg. Chem.* **2003**, *42*, 3396–3398.
[39] K. Mizuoka, Y. Ikeda, *Radiochim. Acta* **2004**, *92*, 631–635.
[40] R. D. Hunt, L. Andrews, *J. Chem. Phys.* **1993**, *98*, 3690–3696.
[41] M. Zhou, L. Andrews, N. Ismail, C. Marsden, *J. Phys. Chem. A* **2000**, *104*, 5495–5502.
[42] X. Wang, L. Andrews, J. Li, B. E. Bursten, *Angew. Chem.* **2004**, *116*, 2608–2611; *Angew. Chem. Int. Ed.* **2004**, *43*, 2554–2557.
[43] D. Majumdar, K. Balasubramanian, H. Nitsche, *Chem. Phys. Lett.* **2002**, *361*, 143–151.
[44] G. S. Groenewold, K. C. Cossel, G. L. Gresham, A. K. Gianotto, A. D. Appelhans, J. E. Olson, M. J. Van Stipdonk, W. Chien, *J. Am. Chem. Soc.* **2006**, *128*, 3075–3084.
[45] A. Fielicke, R. Mitric, G. Meijer, V. Bonacic-Koutecky, G. von Helden, *J. Am. Chem. Soc.* **2003**, *125*, 15716–15717.
[46] J. R. Roscioli, L. R. McCunn, M. A. Johnson, *Science* **2007**, *316*, 249–254.
[47] S. G. Lias, *NIST Chemistry WebBook*, United States Department of Commerce, National Institute of Standards and Technology, Washington, D.C., **2003**, http://webbook.nist.gov/.
[48] M. T. Rodgers, P. B. Armentrout, *Mass Spectrom. Rev.* **2000**, *19*, 215–247.
[49] W. Chien, V. Anbalagan, M. Zandler, D. Hanna, M. Van Stipdonk, G. Gresham, G. Groenewold, *J. Am. Soc. Mass Spectrom.* **2004**, *15*, 777–783.
[50] A. G. Marshall, T.-C. L. Wang, T. L. Ricca, *J. Am. Chem. Soc.* **1985**, *107*, 7893–7897.
[51] V. N. Bagratashivili, V. S. Letokov, A. A. Makarov, E. A. Ryabov, *Mutiple Photon Infrared Laser Photophysics and Photochemistry*, Harwood, Chur, **1985**.
[52] A. G. Marshall, *Acc. Chem. Res.* **1985**, *18*, 316–322.

[53] A. G. Marshall, C. L. Hendrickson, G. S. Jackson, *Mass Spectrom. Rev.* **1998**, *17*, 1–35.
[54] B. Delley, *J. Chem. Phys.* **1990**, *92*, 508–517.
[55] B. Delley, *J. Chem. Phys.* **2000**, *113*, 7756–7764.
[56] E. Aprà et al., *NWChem, A Computational Chemistry Package for Parallel Computers*, Pacific Northwest National Laboratory, Richland, Washington 99352-0999, USA, **2005**.
[57] R. A. Kendall, E. Apra, D. E. Bernholdt, E. J. Bylaska, M. Dupuis, G. I. Fann, R. J. Harrison, J. Ju, J. A. Nichols, J. Nieplocha, T. P. Straatsma, T. L. Windus, A. T. Wong, *Comput. Phys. Commun.* **2000**, *128*, 260–283.
[58] G. te Velde, F. M. Bickelhaupt, E. J. Baerends, C. F. Guerra, S. J. A. Van Gisbergen, J. G. Snijders, T. Ziegler, *J. Comput. Chem.* **2001**, *22*, 931–967.
[59] J. C. Slater, *Phys. Rev.* **1951**, *81*, 385–390.
[60] S. J. Vosko, W. Wilk, M. Nusair, *Can. J. Phys.* **1980**, *58*, 1200–1211.
[61] B. Delley, *Int. J. Quantum Chem.* **1998**, *69*, 423–433.
[62] A. D. Becke, *J. Chem. Phys.* **1993**, *98*, 5648–5652.
[63] C. T. Lee, W. T. Yang, R. G. Parr, *Phys. Rev. B* **1988**, *37*, 785–789.
[64] J. V. Ortiz, P. J. Hay, R. L. Martin, *J. Am. Chem. Soc.* **1992**, *114*, 2736–2737.
[65] T. H. Dunning, *J. Chem. Phys.* **1989**, *90*, 1007–1023.
[66] C. Adamo, V. Barone, *J. Chem. Phys.* **1999**, *110*, 6158–6170.
[67] J. P. Perdew, K. Bruke, M. Emzerhof, *Phys. Rev. Lett.* **1996**, *77*, 3865–3868.
[68] A. Bergner, M. Dolg, W. Kuchle, H. Stoll, H. Preuss, *Mol. Phys.* **1993**, *80*, 1431–1441.
[69] M. Dolg, *Modern Methods and Algorithms of Quantum Chemistry*, John von Neumann Institute for Computing, Julich, **2000**.
[70] T. H. Dunning, Jr., P. H. Hay, *Modern Theoretical Chemistry*, Plenum, New York, **1976**.
[71] W. Küchle, M. Dolg, H. Stoll, H. Preuss, *Mol. Phys.* **1991**, *74*, 1245–1263.
[72] L. F. Pacios, P. A. Christiansen, *J. Chem. Phys.* **1985**, *82*, 2664–2671.
[73] E. van Lenthe, E. J. Baerends, J. G. Snijders, *J. Chem. Phys.* **1993**, *99*, 4597–4610.

Received: January 16, 2008
Revised: April 14, 2008
Published online on May 13, 2008

